

Spike detection approaches for noisy neuronal data: Assessment and comparison



Hamed Azami ^{a,*}, Saeid Sanei ^b

^a Department of Electrical Engineering, Iran University of Science and Technology, Iran

^b Faculty of Engineering and Physical Sciences, University of Surrey, UK

ARTICLE INFO

Article history:

Received 26 July 2012

Received in revised form

18 October 2013

Accepted 2 December 2013

Communicated by Demis Battaglia

Available online 9 January 2014

Keywords:

Spike detection

Fractal dimension

Smoothed nonlinear energy operator

Standard deviation

Empirical mode decomposition

Singular spectrum analysis

ABSTRACT

Spike detection in extracellular recordings is a difficult problem, especially when there are several noise sources. In this paper, three new approaches based on fractal dimension (FD), smoothed nonlinear energy operator (SNEO) and standard deviation to detect the spikes for noisy neuronal data are proposed. These methods however do not perform well in some cases, especially when the noise level is high. To overcome these problems, we use five smoothing techniques, namely, discrete wavelet transform (DWT), Kalman filter (KF), singular spectrum analysis (SSA), Savitzky-Golay filter, and empirical mode decomposition (EMD). Although filtering approach based on EMD is relatively slow, when SNRs > 0 dB, those approaches which use EMD have the best efficiency and accuracy. While SNRs < 0 dB, it is demonstrated that for SSA followed by SNEO, the performance in terms of the average spikes detection accuracy and CPU time is the most desirable.

© 2014 Published by Elsevier B.V.

1. Introduction

Extracellular recordings of neural activity provide a noisy measurement of action potentials produced by a number of neurons adjacent to the recording electrode [1]. Nowadays, multi-site recording techniques such as by using microelectrode arrays (MEAs) for extracellular electrophysiology, with the purpose of investigating the neuronal activity both *in vivo* and *in vitro* have attracted many researchers in neuroscience [2]. The MEAs can answer simultaneous activity of several neurons in an active brain region and answer questions about how the brain works [3]. Unlike scalp electroencephalography (EEG), the neuronal signals recorded using MEAs represent the neural activity directly before being filtered by the nonlinear head tissues and affected by the environment noise.

The problem of nonadditive waveform changes resulting from rapid bursts or slow drift and the detection problem of single or overlapping spikes are two most significant hurdles to the general applicability of unsupervised spike classification methods. The quality of spike detection in the raw electrophysiological signal notably influences the amount and nature of contamination, and thus affects the clustering or classification outcomes [1].

Neural action potentials (also known as nerve impulses or spikes) play an important role in understanding the central nervous system [4,5]. Extracting useful information from these measurements depends on the ability to correctly detect the spikes from the measurements [2]. The environment and measurement noises in one hand and contribution of more than one neuron to each of the recorded spike signal on the other hand are two main problems in spike detection [5,6].

In general, each neuron creates a distinct, reproducible shape, which is then contaminated by noise that can be considered additive. Identified sources of the existing noise contain Johnson noise in the electrode and electronics, background activity of distant neurons, waveform misalignment, electrode micro movement and the variation of the action potential shape as a function of recent firing history. After accounting for non-additive noise sources, the additive noise component is considered as a Gaussian-distributed [1].

There are three main approaches to detect spikes in neural data. The first type includes algorithms that can be implemented in hardware. Amplitude threshold detection is the simplest one of this category. When the signal amplitude exceeds a user-defined threshold, a spike can be discovered. However, this method has a major drawback: its performance is sensitive to the threshold, it is not capable to distinguish between spikes with different morphologies and similar amplitudes, and its performance

* Corresponding author.

E-mail addresses: hmd.azami@yahoo.com (H. Azami),
s.sanei@surrey.ac.uk (S. Sanei).

degrades rapidly when there are many resource noises [7]. In several researches, the mean value or sum of the mean value and standard deviation (or a similar offset value) is proposed as a threshold. If the defined threshold is large, some spikes may not be detected. When the threshold is low, some idle points may be detected as spikes. In this paper we propose three approaches for which the threshold is selected as a mean value of the output signal.

Another widespread method to detect spikes is based on template matching often used in image processing. In this algorithm, the templates representing a typical waveform are used as benchmarks. The first stage of this technique is to select a waveform that represents a typical spike shape as template. In the second stage, the method locates possible events in the signal that “closely resemble” the template; and, finally, there is a thresholding stage. Early techniques often started with the experimenter identifying a number of good spikes, and using them to train a filter. However, this is impractical, especially when there are large numbers of electrodes [7,8]. Although the template matching algorithm often detects spike events better than simple threshold algorithms, this improved performance depends on a priori knowledge of the spike shape to form the template. Also, since the automatic selection of a template in a noisy signal is very difficult, the performance of the method decreases in low SNR [7,8].

The third approach uses signal transformations such as non-linear energy operator (NEO or NLEO) [7,9]. Although NEO is a powerful tool for spike detection, when there is a multi-frequency or multi-component signal, the output of the NEO includes a DC part and the time-varying part called cross-terms. These cross-terms and noises decrease the accuracy of spike detection [8]. To overcome these problems, in this paper we use the smoothed NEO (SNEO) to detect the spikes in neuronal data.

Mtetwa and Smith have presented five spike detection techniques and three thresholding criteria for spike detection. The best method between these methods was based on normalized cumulative energy difference (NCED). This method inspired by the fact that the energy in a spike (positive or negative going) should be greater than that in noise of the same length can be followed by multi-template-based spike sorting, and it is amenable to implementation in digital electronics for neural real-time processing [3].

The changes in fractal dimension (FD) refer to the underlying statistical variations of the signals and time series including the transients and sharp changes in both amplitude and frequency. Since spike is a part of a signal that its amplitude and frequency is considerably different with other parts of a signal, FD can be used as a spike detector. There are several methods to compute the FD of a signal such as Petrosian's, Hiaguchi's, and Katz's methods. Although Hiaguchi's method computes the FD more precisely than Katz's method, due to high sensitivity of Hiaguchi's method to noises, Katz's method is often used in signal processing applications [10]. Note that we tested all three FD methods and chose Katz's method as the best one.

We have used the standard deviation to detect segmentation boundaries (not spike detection) of the signal and have shown that the standard deviation can be used as a detector for changes of the amplitude and/or frequency of a signal [11]. Since in spikes, amplitude and frequency significantly change, in this paper we propose the standard deviation for detecting the spikes in neuronal signals. Like two other proposed methods, standard deviation is very sensitive to noises.

Time series measured in real world is commonly nonlinear and in order to reduce noises or extract significant information from the measured time series, it is important to use pre-processing steps such as wavelet transform and filters [12]. Therefore, in this

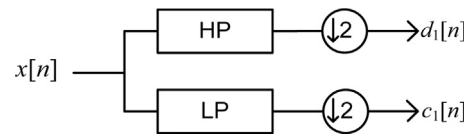


Fig. 1. Estimation of DWT coefficients using lowpass and highpass filtering followed by decimation.

paper, discrete wavelet transform (DWT) as pre-processing step is applied for all of the mentioned methods. Although DWT is a powerful tool to attenuate noises, the speed of the method is almost high. To overcome this problem, Savitzky–Golay filter, singular spectrum analysis (SSA), Kalman filter (KF), and Empirical mode decomposition (EMD) are proposed.

Savitzky–Golay filter is an effective tool for de-noising and smoothing signals [13]. Compared with moving average (MA) filter, Savitzky–Golay tends to keep features of the distribution such as relative with maxima and minima [13]. SSA is becoming an effective and powerful tool for time series analysis in meteorology, hydrology, geophysics, climatology, economics, biology, physics, medicine, and other sciences where short and long, one-dimensional and multi-dimensional, stationary and non-stationary, almost deterministic and noisy time series are to be analyzed [14].

Real data often includes noise; this noise deteriorates the spike detection procedure. To better avoid the noise effect, KF is used in this article. KF is an efficient recursive filter that predicts the state of a dynamic system from a series of measurements with error. On the other hand, EMD is a powerful and new method applied to decompose the data into a number of intrinsic mode functions (IMFs) and a residual signal from a complex time series [15]. While each IMF has almost a specific frequency with mean value of zero, each IMF can be considered as a noise signal originated from a special and unknown source. Thus, the residual signal is a filtered version of the original signal combined with a number of noise sources.

In the next section DWT, Savitzky–Golay filter, SSA, KF, EMD, and FD are briefly reviewed. **Section 3** explains the three proposed methods. **Section 4** provides introduction on the dataset used in this paper and then, the comparison between the results of the proposed methods are presented. The last section concludes the paper.

2. Background knowledge for the proposed methods

2.1. Preprocessing

Traditionally, DWT has been employed in denoising various data. It has been widely used in analysis of biological signals and time series including brain signals [16,17]. DWT decomposes a signal into different scales with different level of resolutions. Majority of signal information is located within lower frequency components and carry the major information. DWT coefficients are estimated simply by lowpass and highpass filtering the data $x[n]$ as in Fig. 1 [18], where $d_1(n)$ and $c_1(n)$ are the first level DWT coefficients [19]. DWT is known as a time consuming time algorithm. Therefore, in what follows three new methods are presented. The first method, Savitzky–Golay filter, is a smoothing method which best fits to the data fluctuation. DWT may not perform well for the cases where the data has flat temporal or spectral characteristics. The second and third methods i.e. SSA and KF are a data-dependent and flexible method which can be adapted to the data. Furthermore, parameters of DWT, SSA, KF,

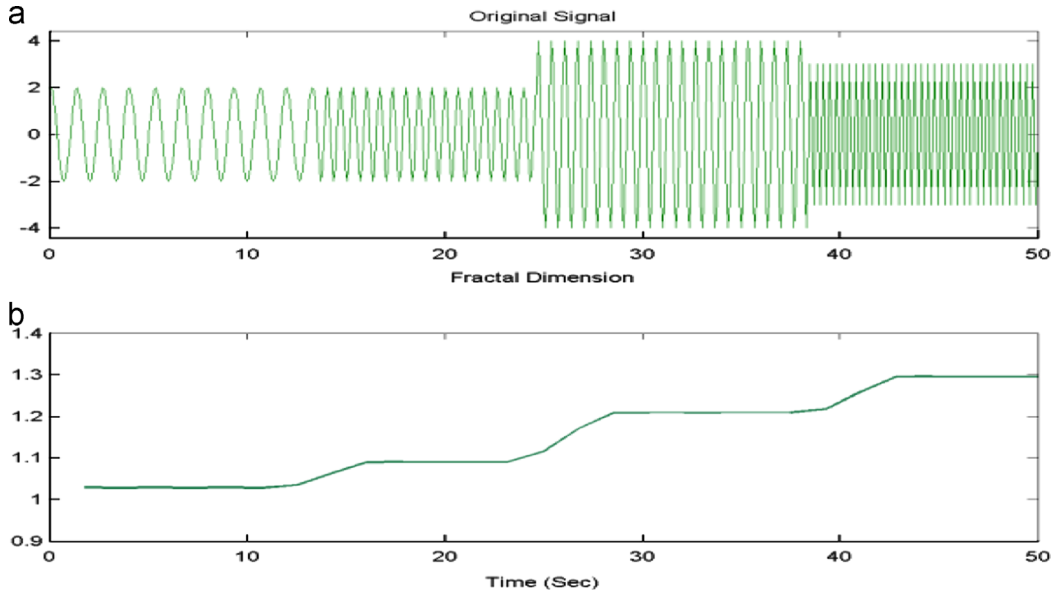


Fig. 2. Variation of FD when amplitude or frequency changes.

and Savitzky–Golay filter must be adjusted empirically. To overcome this problem we use an approach based on EMD. These methods are described below in detail and their results compared with those of DWT.

2.1.1. Savitzky-Golay filter

The Savitzky–Golay filter is a powerful tool for smoothing a signal proposed by Savitzky and Golay in 1964. The filter is defined as a weighted moving average with weighting given as a polynomial of specific degree [20–22]. The coefficients of a Savitzky–Golay filter, when applied to a signal, perform a polynomial P of the degree k , is fitted to $N = N_r + N_l + 1$ points of the signal, where N is the window size and N_r and N_l are signal points in the right and left of a current signal point, respectively. One of the best advantages of this filter is that it tends to keep the distribution features such as maxima and minima which are often flattened by other smoothing techniques such as the moving average (MA) filters [20–22]. This property makes the Savitzky–Golay filter a favorable tool to detect the spikes.

2.1.2. Singular spectrum analysis

In this subsection a brief description of the two SSA stages together with the corresponding mathematics is given. At the first stage, the series is decomposed and at the second stage we reconstruct the original series and use the reconstructed series (which is without noise) to predict new data points [23].

- (1) Decomposition: this stage is composed of two sequential steps including embedding and singular value decomposition (SVD). In the embedding step, the time series s is mapped to k dimensional lagged vectors of length l as follows:

$$x_i = [s_{i-1}, s_i, \dots, s_{i+l-2}]^T, \quad 1 \leq i \leq k \quad (1)$$

where $k = r - l + 1$, l is the window length ($1 \leq l \leq r$), and $[]^T$ denotes the transpose of a matrix. An appropriate window length totally depends on the application and the prior information about the signals of interest. The trajectory matrix of the series \mathbf{s} is constructed by inserting each \mathbf{x}_i as the i th

column of an $l \times k$ matrix, i.e.

$$\mathbf{X} = [\mathbf{x}_1, \mathbf{x}_2, \dots, \mathbf{x}_k] = \begin{bmatrix} s_0 & s_1 & s_2 & \dots & s_{k-1} \\ s_1 & s_2 & s_3 & \dots & s_k \\ s_2 & s_3 & s_4 & \dots & s_{k+1} \\ \vdots & \vdots & \vdots & \ddots & \vdots \\ s_{l-1} & s_l & s_{l+1} & \dots & s_{r-1} \end{bmatrix} \quad (2)$$

Note that the trajectory matrix \mathbf{X} is a Hankel matrix, i.e. for all the elements along its diagonals $i+j=\text{constant}$.

In the SVD substage, the SVD of the trajectory matrix is computed and represented as the sum of rank-one biorthogonal elementary matrices. Consider the eigenvalues and corresponding eigenvectors of $\mathbf{S} = \mathbf{X}\mathbf{X}^T$ are $\lambda_1, \lambda_2, \dots, \lambda_l$ and $\mathbf{e}_1, \mathbf{e}_2, \dots, \mathbf{e}_l$, respectively. If $\mathbf{v}_i = \mathbf{X}^T \mathbf{e}_i / \sqrt{\lambda_i}$, then the SVD of the trajectory matrix can be written as

$$\mathbf{X} = \mathbf{X}_1 + \mathbf{X}_2 + \dots + \mathbf{X}_d \quad (3)$$

where $d = \text{argmax}_i \{ \lambda_i > 0 \}$ and $\mathbf{X}_i = \sqrt{\lambda_i} \mathbf{e}_i \mathbf{v}_i^T$. The i th eigen-triple of the SVD decomposition comprises of \mathbf{v}_i , \mathbf{e}_i , and λ_i . Projecting the time series onto the direction of each eigenvector yields the corresponding temporal principal component [14].

- (2) Reconstruction: this stage has two steps: grouping and diagonal averaging. (a) Grouping averaging: this step divides the set of indices $\{1, 2, \dots, d\}$ to m disjoint subsets I_1, I_2, \dots, I_m . For every group $I_j = \{i_{j1}, i_{j2}, \dots, i_{jp}\}$, we have $\mathbf{X}_{I_j} = [X_{i_{j1}}, X_{i_{j2}}, \dots, X_{i_{jp}}]$. Grouping the eigentriples and expanding all matrices \mathbf{X}_{I_j} , Eq. (3) can be written as

$$\mathbf{X} = \{\mathbf{X}_{I_1}, \mathbf{X}_{I_2}, \dots, \mathbf{X}_{I_m}\} \quad (4)$$

There is no general rule for grouping. For each application, the grouping rule depends on the special requirements of the problem and the type of the contributing signals and noise.

(b) Diagonal averaging: in the final stage of analysis, each group is transformed into a series of length r . For a typical $l \times k$ matrix \mathbf{Y} , the q th element of the resulted time series, g_q is calculated by averaging the matrix elements over the diagonal $i+j=q+2$, where i and j are the row and column indices of \mathbf{Y} , respectively [23,24].

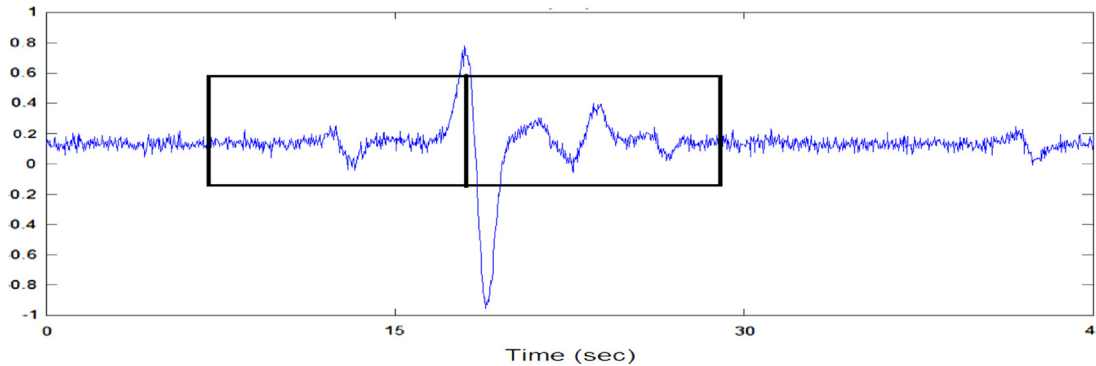


Fig. 3. Illustration of joint sliding windows along the time.

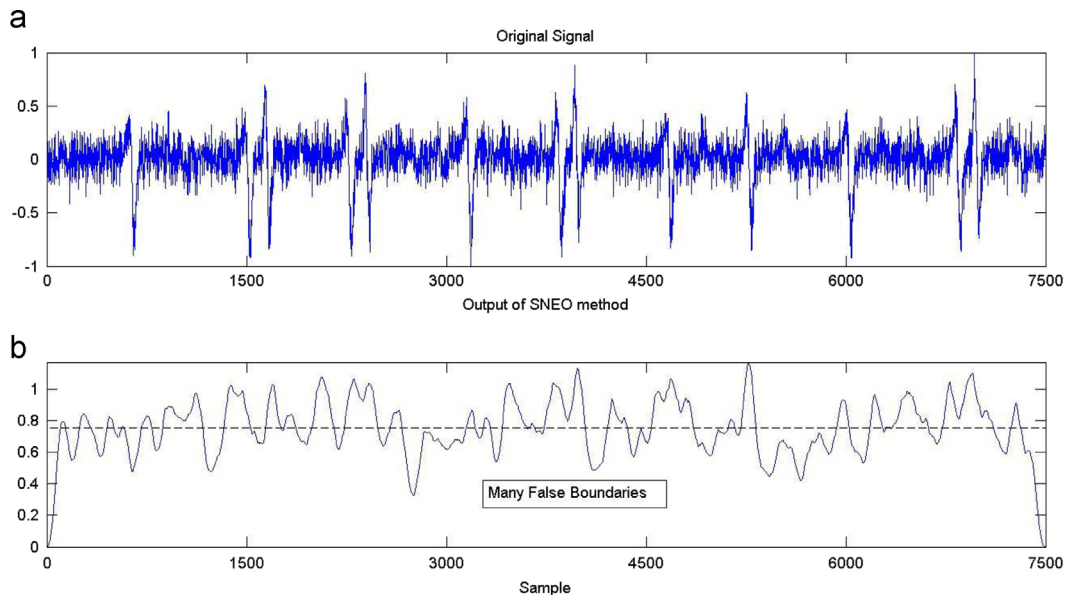


Fig. 4. Spike detection in semi real EEG signal using SNEO; (a) original signal, and (b) output of the SNEO method.

The concept of separability is an important part of the SSA methodology. Assume that s is the sum of two series s_1 and s_2 , i.e., $s = s_1 + s_2$. Separability means that the matrix terms of the SVD of the trajectory matrix of X can be divided into two disjoint groups, such that the sums of the terms within the groups result in the trajectory matrices X_1 and X_2 of the time series s_1 and s_2 , respectively [24]. A necessary condition for separability of the sources is disjointedness of their frequency spectrum. It is also worth mentioning that exact separability cannot be achieved for real-world signals; hence, only approximate separability can be considered.

The eigentriples resulting from the SSA also contain information about the frequency content of the data. If there is a periodic component in the data, it will be reflected in the output of the SSA as a pair of (almost) equal eigenvalues [23,24]. Moreover, the highest peaks in the Fourier transform of the corresponding eigenvectors are related to the frequency of the periodic component. These features of the SSA are used to construct data-driven filters [23,24].

2.1.3. Kalman filter

KF is a powerful recursive algorithm that approximates the state of a dynamic system linearly from a signal sequence [25–27]. It is mainly applied for solving two major problems (I) reducing noises and (II) tracking the changes in the state of linear systems [28,29]. The KF works in two stages: first stage is prediction and

the second is correction. In the first stage, the system state is predicted using a dynamic model. In the second stage the model is corrected with the help of the observation sequence. During this process the covariance of the approximation error is minimized [28,29].

2.1.4. Empirical mode decomposition

As mentioned before, EMD is a powerful and new method applied to decompose the IMFs from a complex time series. This decomposition, so called sifting process, uses the mean of the upper and lower envelopes. The sifting process must be repeated until every component satisfies two conditions [30,31]

- (1) The number of extrema and the number of zero-crossings must either be equal or differ at most by one.
- (2) At any point, the mean value of the two envelopes defined respectively by local maxima and local minima must be zero.

For an arbitrary time series $x(t)$, the sifting process can be summarized as follows:

- (1) Identify all the local extrema (maxima or minima) of signal $x(t)$, and then connect all the local maxima by a cubic spline line (upper envelope).
- (2) Repeat similarly for all the local minima (lower envelope).

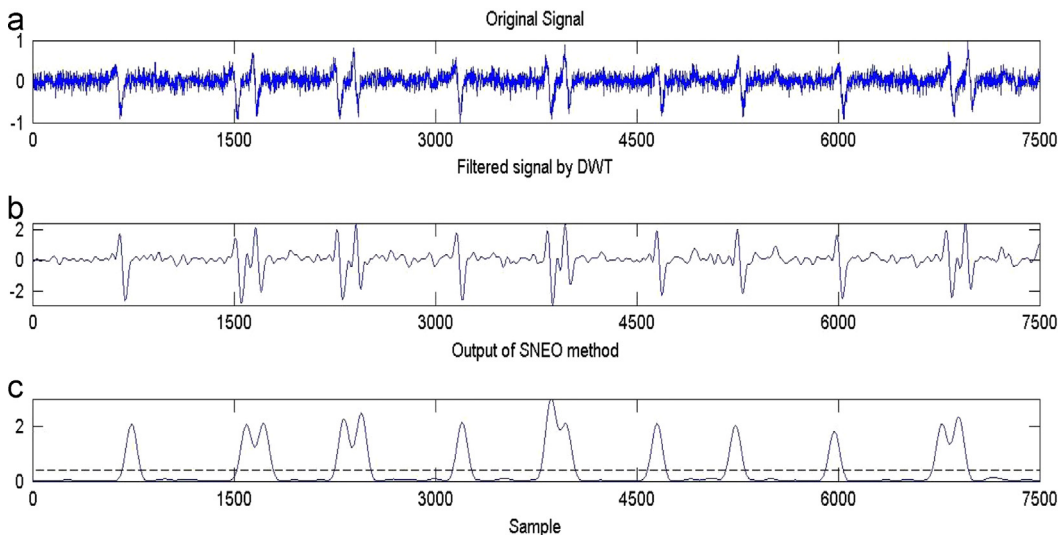


Fig. 5. Spike detection in test signal using the SNEO and DWT; (a) original signal, (b) decomposed signal after applying four-level DWT, and (c) output of the SNEO method. It can be seen that all 13 spikes can be accurately detected.

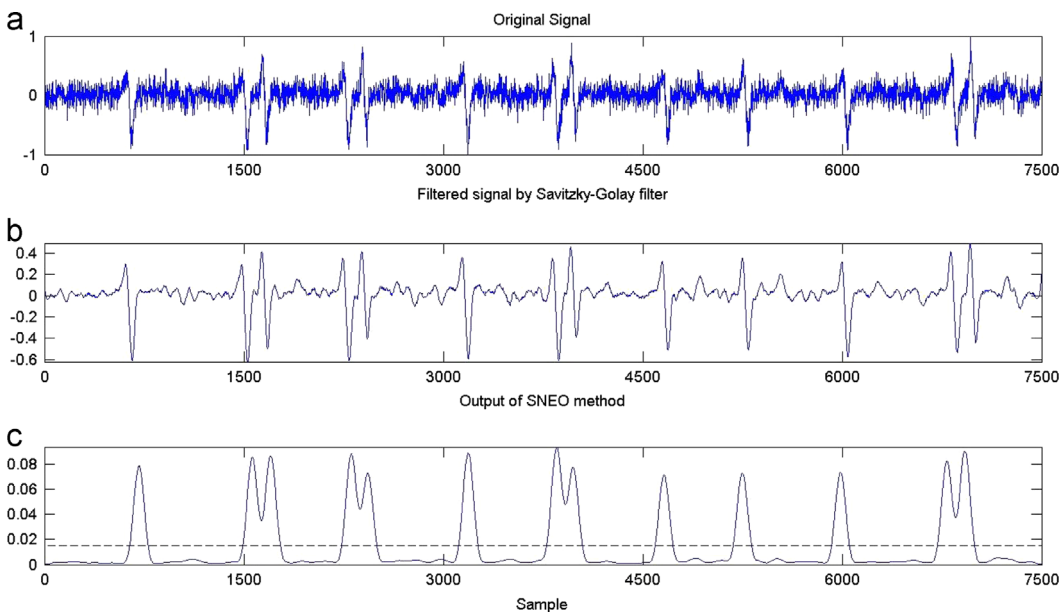


Fig. 6. Spike detection in test signal using the SNEO and Savitzky-Golay filter; (a) original signal, (b) filtered signal by Savitzky-Golay, and (c) output of the SNEO method. It can be seen that all 13 spikes can be accurately detected.

(3) The mean of the upper and lower envelopes is designated as $m(t)$. The difference between the data and $m(t)$ is the first component as follows:

$$h_1(t) = x(t) - m(t). \quad (5)$$

(4) Consider $h_1(t)$ as the new original signal and repeat above steps.

Generally, this process must be repeated until the last $h_1(t)$ has at most one extrema or becomes constant. It is nearly impossible to achieve a mean spline that is exactly zero for the signal's duration, so a final stopping criterion have to be set to determine the instant when the sifting process results in an IMF. This criterion is a predetermined RMS tolerance between two consecutive components of sifting. Thus, in this paper we use the criterion applied in [32].

2.2. Fractal dimension

FD is a measure of nonlinear dynamics of time series and has recently become popular in analysis of biomedical signals such as EEG [33,34]. If the amplitude and frequency of a signal change, the dimension of FD will change the same as Fig. 2.

The synthetic signal used here includes four segments. The first and second segments have the same amplitude. The frequency of the first part is however different from that of the second part. In the third segment the amplitude becomes different from that of the second segment. Amplitude and frequency in the 4th segment is different from that of the third segment. The reason for creating this signal is to show that if two adjacent epochs of a signal have different amplitudes and/or frequencies, the FD will vary.

There are some methods to calculate the FD of a signal such as Hiaguchi, Petrosian, and Katz's methods [10]. Because FD is directly estimated from the time-varying signal, it has low computational

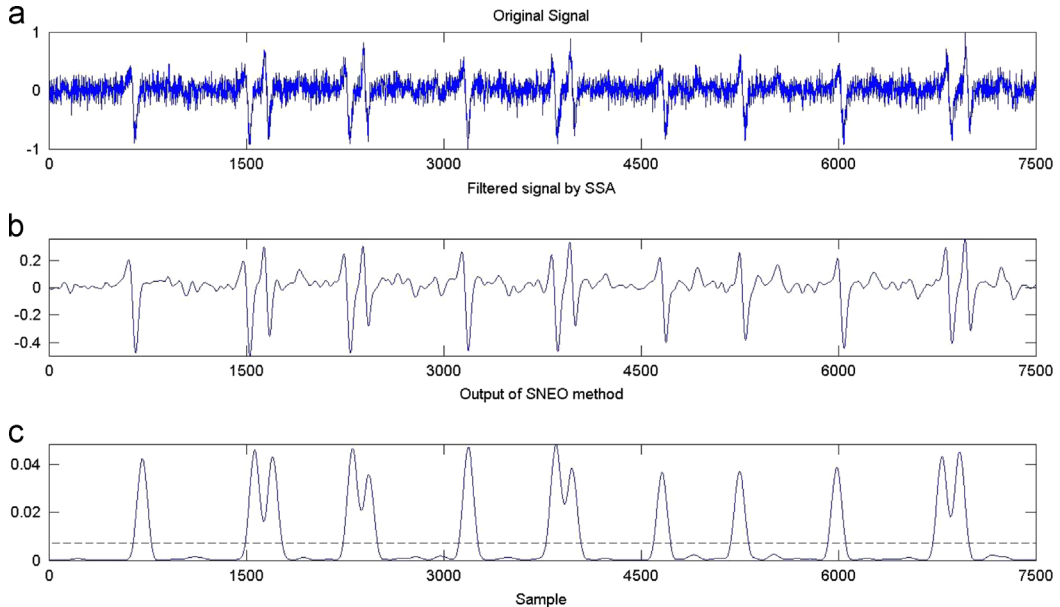


Fig. 7. Spike detection in test signal using the SNEO and SSA; (a) original signal, (b) filtered signal by SSA, and (c) output of the SNEO method. It can be seen that all 13 spikes can be accurately detected.

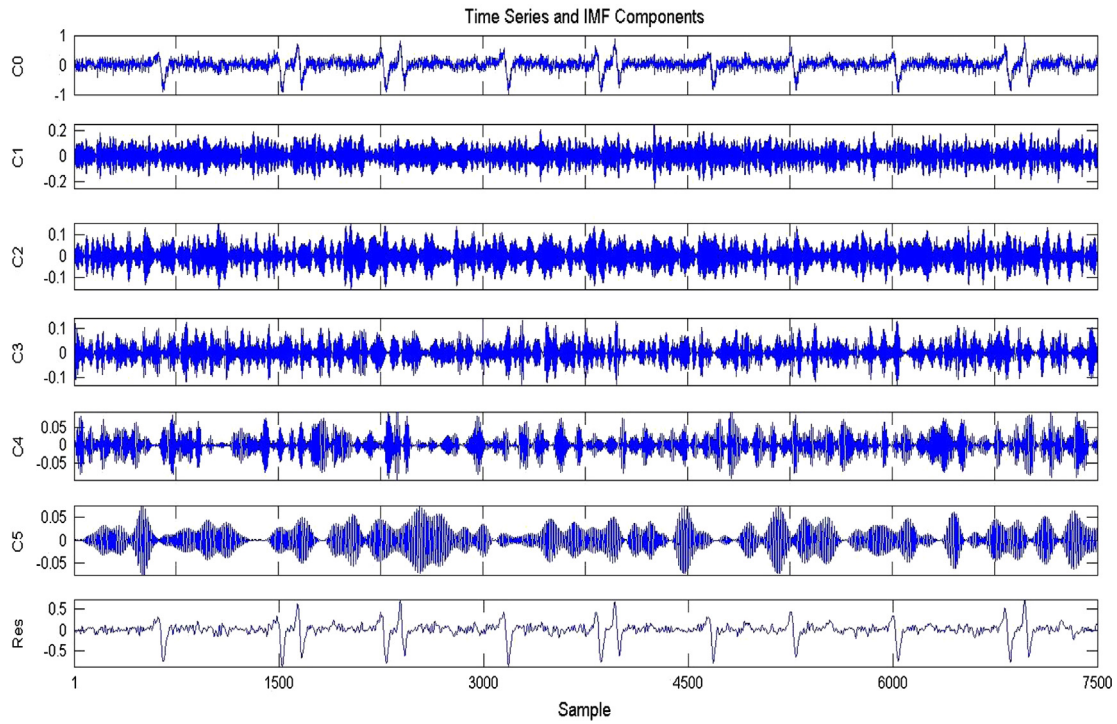


Fig. 8. Components of the restored realistic synthetic signal by EMD. The first time series is the filtered signal. The decomposition yields 5 IMF and a residual. The IMFs are the time-frequency constituents or components of the realistic synthetic neuronal signal.

cost. Katz's algorithm has a lower sensitivity to noise and good speed in contrast to the two other algorithms [10]. Using Katz's algorithm

$$FD = \frac{\log_{10}(n)}{\log_{10}(d/L) + \log_{10}(n)} \quad (6)$$

where L is the sum of the distances between consecutive points and d is the maximum distance between the first point of the time series and the point that has maximum distance from it. Also, $n=L/a$ shows the step size in the time series [10].

3. Proposed methods

In the following subsections three new methods for neuronal data spike detection have been proposed.

3.1. Spike detection using improved smoothed nonlinear energy operator

Kaiser has suggested an operator, NEO, to measure the instantaneous energy of the signal as follows [35]:

$$\psi[x(n)] = x^2(n) - x(n-1)x(n+1) \quad (7)$$

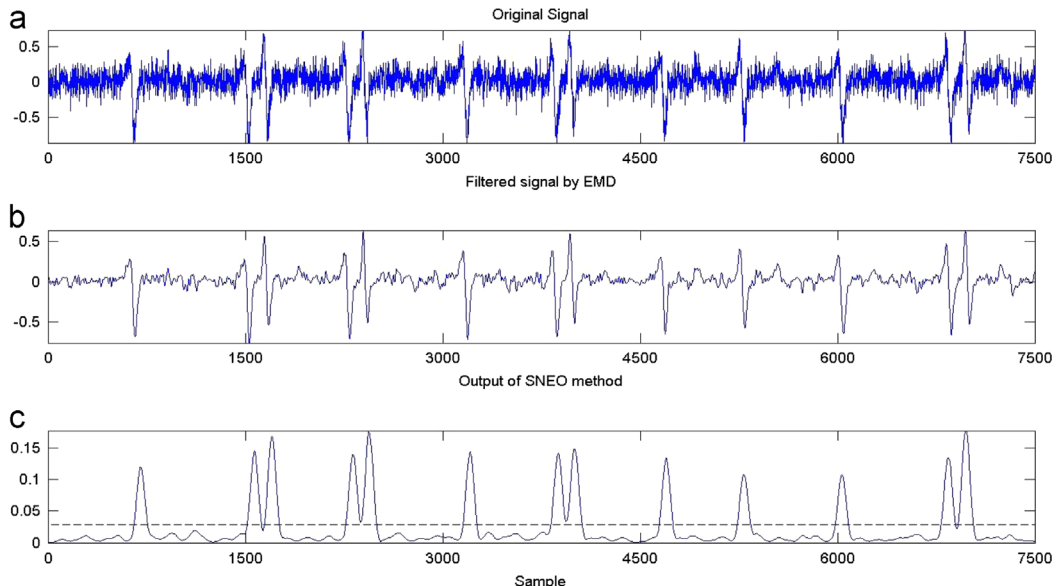


Fig. 9. Spike detection in test signal using the SNEO and EMD; (a) original signal, (b) filtered signal by EMD, and (c) output of the SNEO method. It can be seen that all 13 spikes can be accurately detected.

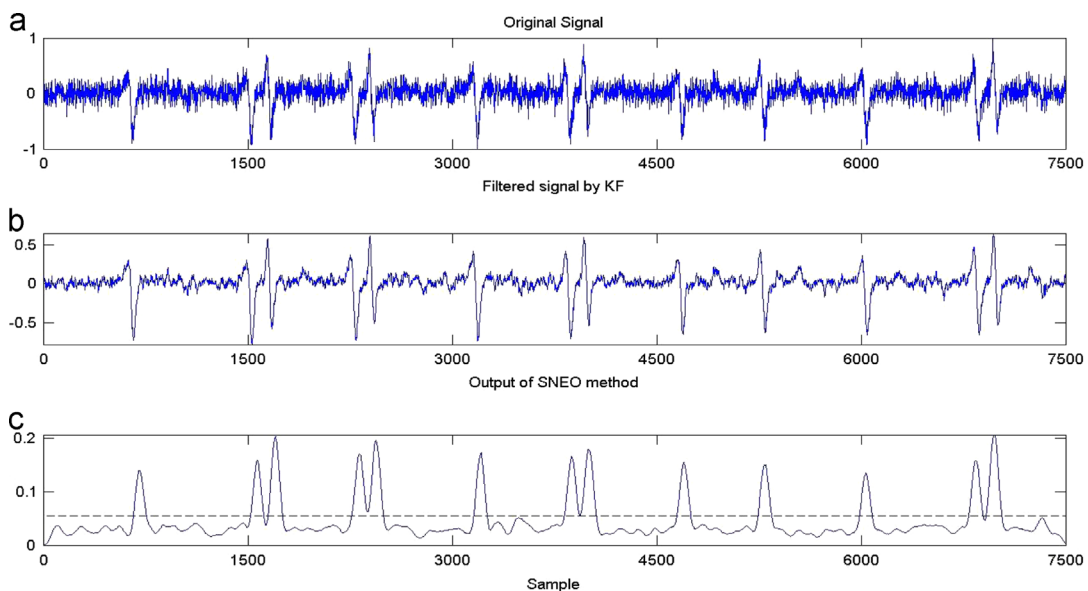


Fig. 10. Spike detection in test signal using the SNEO and KF; (a) original signal, (b) filtered signal by KF, and (c) output of the SNEO method. It can be seen that all 13 spikes can be accurately detected.

If the $x(n)$ is a sinusoidal wave, then, $\psi[x(n)]$ will be defined as

$$Q(n) = \psi[A\cos(\omega_0 n + \theta)] = A^2 \sin^2 \omega_0 \quad (8)$$

when ω_0 is much smaller than the sampling frequency, then, $Q(n) = A^2 \omega_0^2$. In other words, the operator can detect changes in the instantaneous amplitude (A) or instantaneous frequency (ω_0) of the signal [36]. Therefore, the NEO can be used for amplifying the spiky activities in a signal. However, the NEO is sensitive to noise and has the problem of cross terms operator [36]. To reduce these problems, Mukhopadhyay and Ray have suggested SNEO to detect spike events in EEG signals by convolving $\psi[x(n)]$ with a time domain window expressed as

$$\psi_S[x(n)] = w(n) * \psi[x(n)] \quad (9)$$

where $*$ denotes convolution operator and $w(n)$ shows the window. The choices of window type and width of the window are very important to achieve sufficient reduction of interference without losing much of its time resolution which it is very important for spike detection. In order to achieve this aim, Bartlett window function with an integer filter implementation was selected to hold the complexity of the algorithm as low as possible [9].

The local optimum from the output of the SNEO that is higher than a predefined threshold, Tr , is selected as a spike at that location in the time series. A threshold as a scaled version of the mean of the output filter is defined as follows:

$$Tr = c \frac{1}{N} \sum_{n=1}^N \psi_S[x(n)] \quad (10)$$

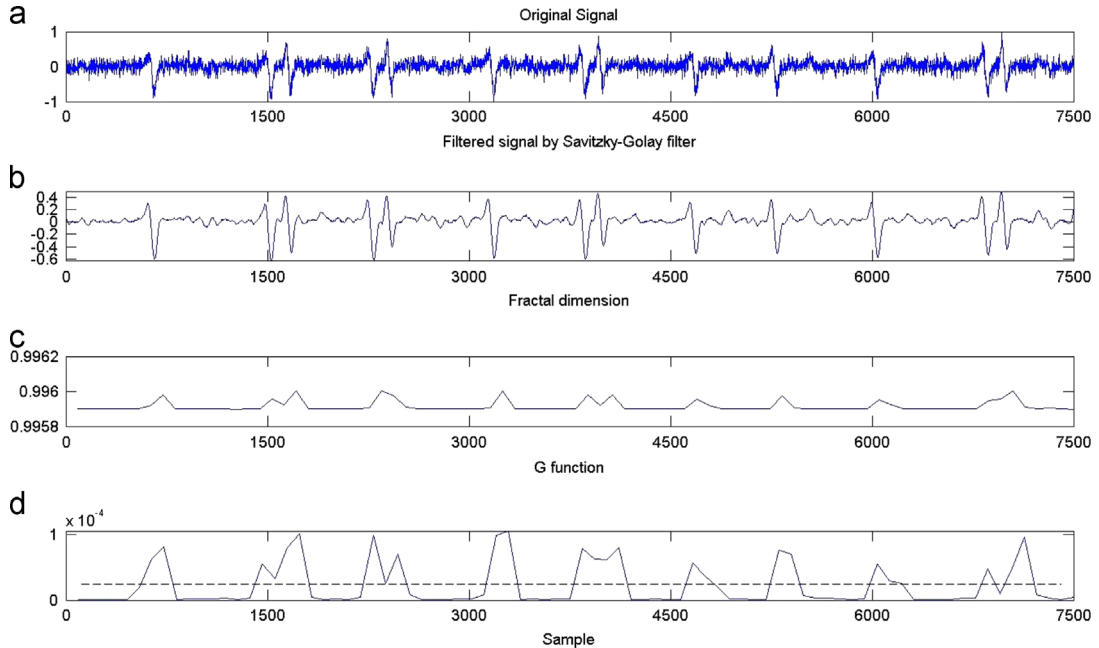


Fig. 11. Spike detection in test signal using FD and Savitzky–Golay filter; (a) original signal, (b) filtered signal by Savitzky–Golay, (c) output of FD, and (d) G function result.

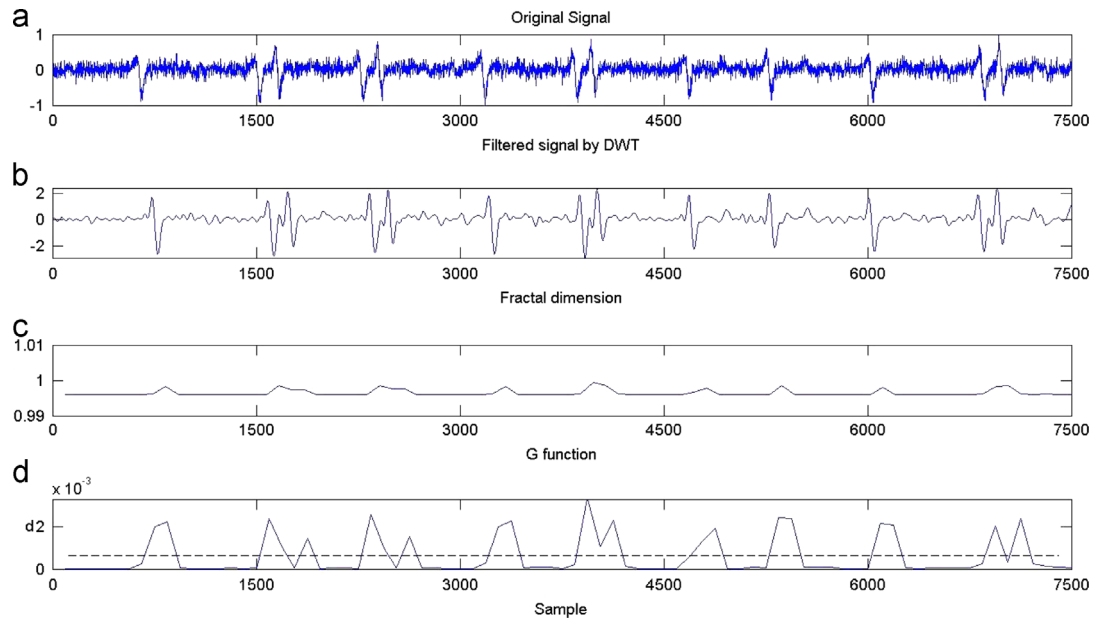


Fig. 12. Spike detection in the test signal using the FD and DWT; (a) original signal, (b) decomposed signal after applying four-level DWT, (c) output of FD, and (d) G function result. It can be seen that all 13 spikes can be accurately detected.

where N is the number of samples and c is a scaling factor. Before implementing the above threshold, for a pre-selected signal the scaling factor “ c ” is adjusted by trial and error and used as a constant. However, the SNEO method is still sensitive to noise [36]. Therefore, using a filter or smoother in the pre-processing stage can significantly increase the performance of this method. The SNEO has been employed in this application for the first time.

3.2. Spike detection using fractal dimension

In this method, two windows slide along the signal like in Fig. 3 and for each window the FD is calculated with the Katz's algorithm

to find the spikes of the signal. The FD variations are computed as

$$G_t = |FD_{t+1} - FD_t|, \quad t = 1, 2, \dots, L-1 \quad (11)$$

where t is the number of analyzing window and L is the total number of windows. Unlike in previous method, here, the threshold is defined as the mean value in the distribution. When the local maxima of G are bigger than the threshold, these times are chosen as the spikes' locations within the signal.

3.3. Spike detection using standard deviation

In this method like spike detection method with FD, two similar scrolling windows move along the signal. For each window,

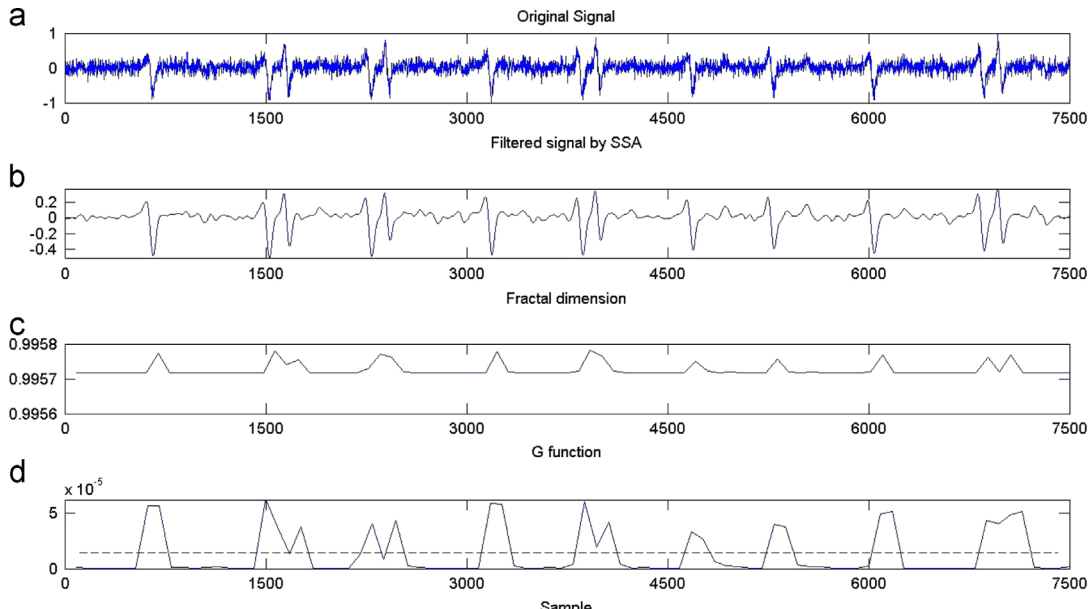


Fig. 13. Spike detection in test signal using FD and SSA; (a) original signal, (b) filtered signal by SSA, (c) output of FD, and (d) G function result. It can be seen that all 13 spikes can be accurately detected.

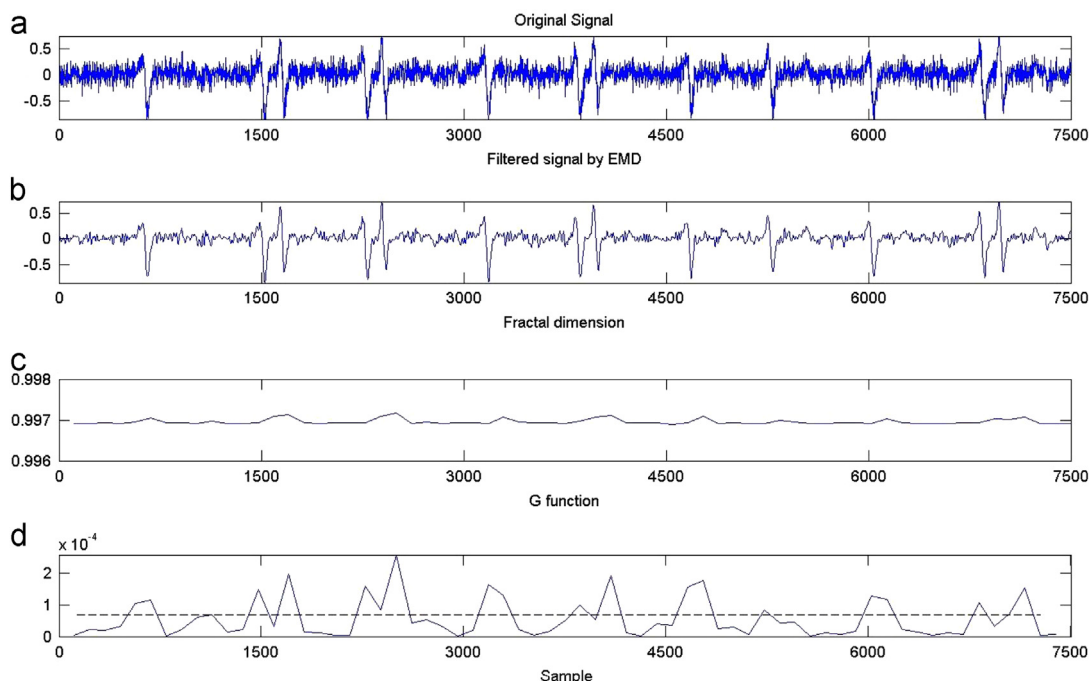


Fig. 14. Spike detection in test signal using FD and EMD; (a) original signal, (b) filtered signal by EMD, (c) output of FD, and (d) G function result. It can be seen that all 13 spikes can be accurately detected.

the standard deviation is computed. H function is used to detect spikes of the signal as follows:

$$H_a = |std_{a+1} - std_a|, \quad a = 1, 2, \dots, m-1 \quad (12)$$

where a and m are the number of analyzed window and the total number of analyzed windows, respectively. std_a denotes the standard deviation of a part of the signal which is located in the a th analyzed window. If the local maximum is bigger than the threshold, the mean value of H_a , the current time is selected as a spike of the signal.

4. Simulation results

As stated before, to enhance the performance of the presented methods, we examine KF, SSA and Savitzky-Golay filter as pre-processing steps and compare them with DWT. Because of the lack of ground truth data (i.e., spike timings for each neuron) spike detection methods are often difficult to evaluate. In [37] generation and transmission of intracellular signals from neurons to an extracellular electrode have been modeled and a set of MATLAB functions based on this analysis provided. The codes have been used here to generate a set of realistic synthetic neural data. They produce realistic signals

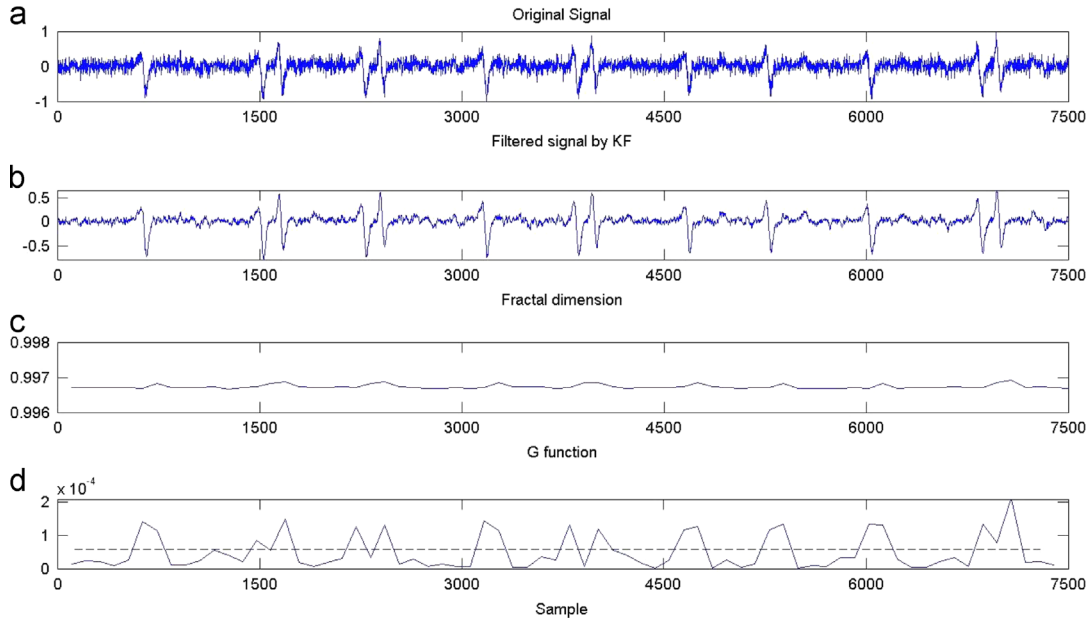


Fig. 15. Spike detection in test signal using FD and KF; (a) original signal, (b) filtered signal by KF, (c) output of FD, and (d) G function result. It can be seen that all 13 spikes can be accurately detected.

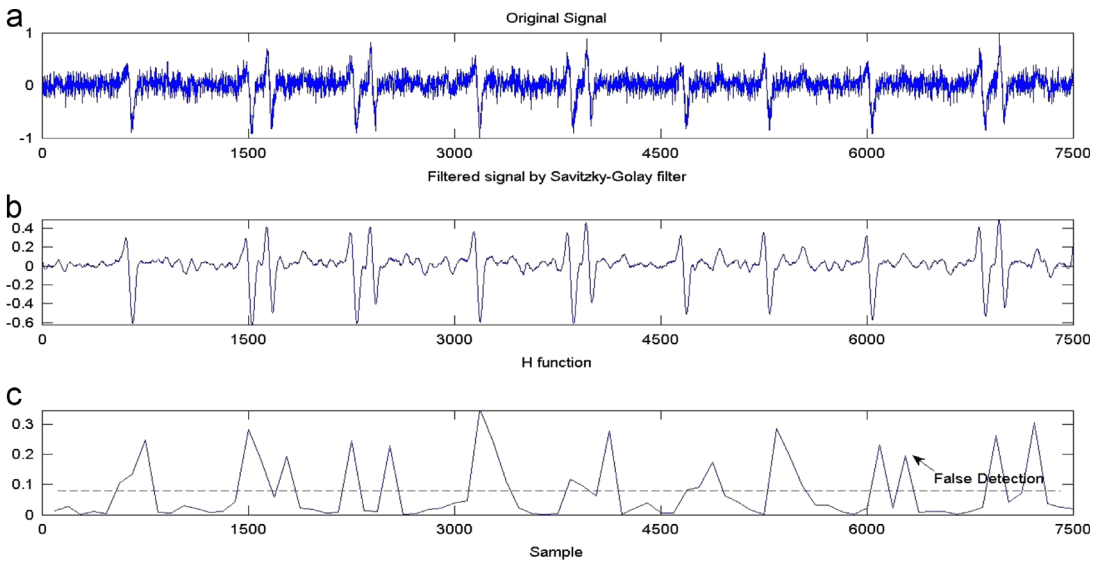


Fig. 16. Spike detection in test signal using standard deviation and Savitzky-Golay filter; (a) original signal, (b) filtered signal, and (c) H function result.

from a set of nearby neurons including interference from more distant neurons and Gaussian noise. These data best resemble the output of deep mesio-temporal brain discharges observed at cortical electrodes. Also, In [37] it has mentioned that there are the correlated and uncorrelated spike noises in neuronal data as well as some Gaussian noise; In order to follow this we simulated the effect of thermal and amplifier noise. Correlated spike noise is created by linearly mixing the differentiated jittered spike sequence and twice the differentiated jittered spike sequence. Uncorrelated spike noise is created by linearly mixing the differentiated uncorrelated spike sequence and twice the differentiated uncorrelated spike trains created. After considering these kinds of noise sources, the noise component is added as a Gaussian-distributed.

By following this synthesizing method, we have randomly generated 70 realistic synthetic neuronal data each including

Gaussian noise with $\text{SNR} = -5, 0, 5, 10, 20$ and 50 dBs. For each SNR level, each data contains 12–14 spikes. Therefore, we have about $70 \times 6 \times 13 = 5460$ spikes to test. One of 70 signals that contains 13 spikes with $\text{SNR} = 5$ dB is randomly selected as the test signal. This signal is shown in Fig. 4(a). The output of the SNEO method is shown in Fig. 4(b). The scaled factor and window length are selected 1 and 400 samples, respectively. These parameters are selected after many trials. As can be seen in Fig. 4 the SNEO cannot properly detect the spikes.

The test signal in Fig. 5(a) is initially decomposed using four-level DWT. In this paper we used the DWT with Daubechies wavelet of order eight. This decomposed signal is shown in Fig. 5(b). As we can see, the decomposed signal is smoother than the original signal. Fig. 5(c) shows the output of the SNEO method. The Savitzky–Golay filter is applied for the test signal in Fig. 6.

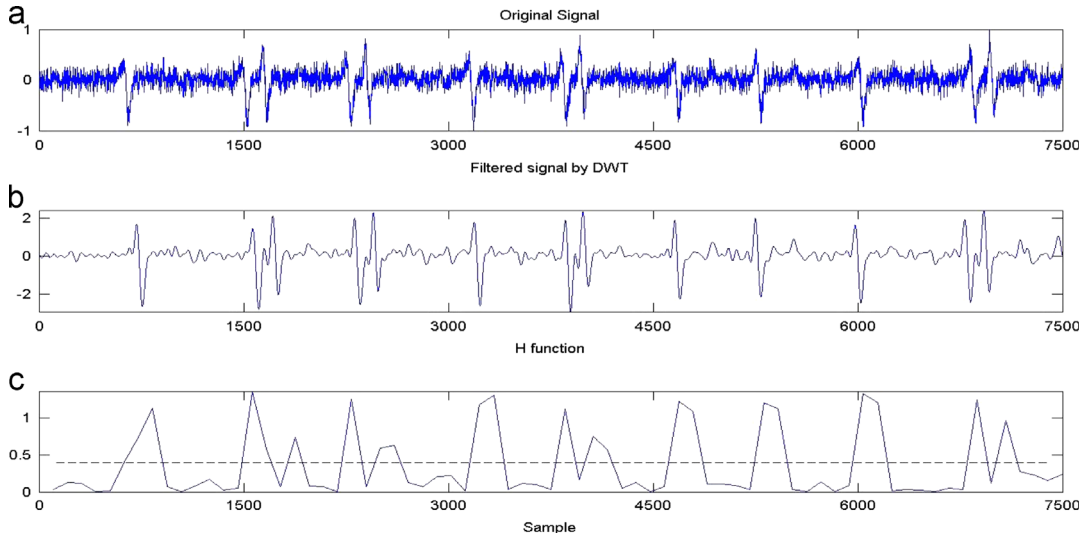


Fig. 17. Spike detection in test signal using standard deviation and DWT; (a) original signal, (b) decomposed signal after applying four-level DWT, and (c) H function result. It can be seen that all 13 spikes can be accurately detected.

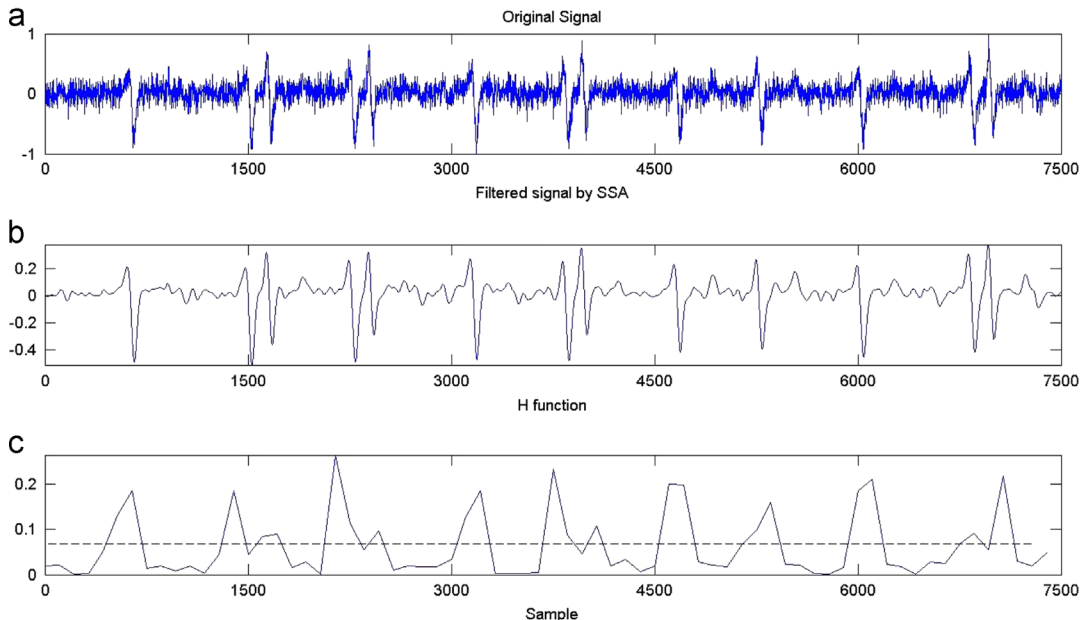


Fig. 18. Spike detection in test signal using standard deviation and SSA; (a) original signal, (b) decomposed signal after applying SSA, and (c) H function result. It can be seen that all 13 spikes can be accurately detected.

The result is shown in Fig. 6(c). In this paper, we have used an order three polynomial Savitzky–Golay filter. A frame size of 51 samples was chosen for the filter. Fig. 7(c) shows the output of the SNEO method by using SSA as a pre-processing step.

SSA, like many filters, has an important short-coming, i.e. there are several parameters to be adjusted using a large number of trials. The filtering process for a particular signal is sensitive to selection of these parameters. When l and l' are selected too large, some important information of the original signal is removed by this filter. For too small l and l' , however, this filter cannot attenuate destructive noises sufficiently. We should try to make a trade-off between these two limitations. Also, for SSA the embedding dimension should be larger than twice the longest cycle period of the data. The number of selected eigenvalues depends on the complexity of the desired component. The SSA

used for this paper has window length equal to 20 that is selected with trial and error.

In this paper we propose to employ EMD to reduce the noise. As stated before, the residual signal obtained by EMD can be considered as a filtered signal extracted from an original signal combined with some noise sources with mean values of zero. In Fig. 8 we can see the result of decomposition performed by EMD of the filtered test signal. This figure illustrates that the first mode has a higher frequency than the second mode where modes are ordered from highest to lowest frequencies. Fig. 9(c) shows the outcome of using EMD and SNEO for the test signal. The very important advantage of employing EMD is that unlike usual filters, EMD does not need any adjustment of parameters.

In Fig. 10(a and b) the test data described above and the filtered signal by KF are shown, respectively. As we can see, the filtered

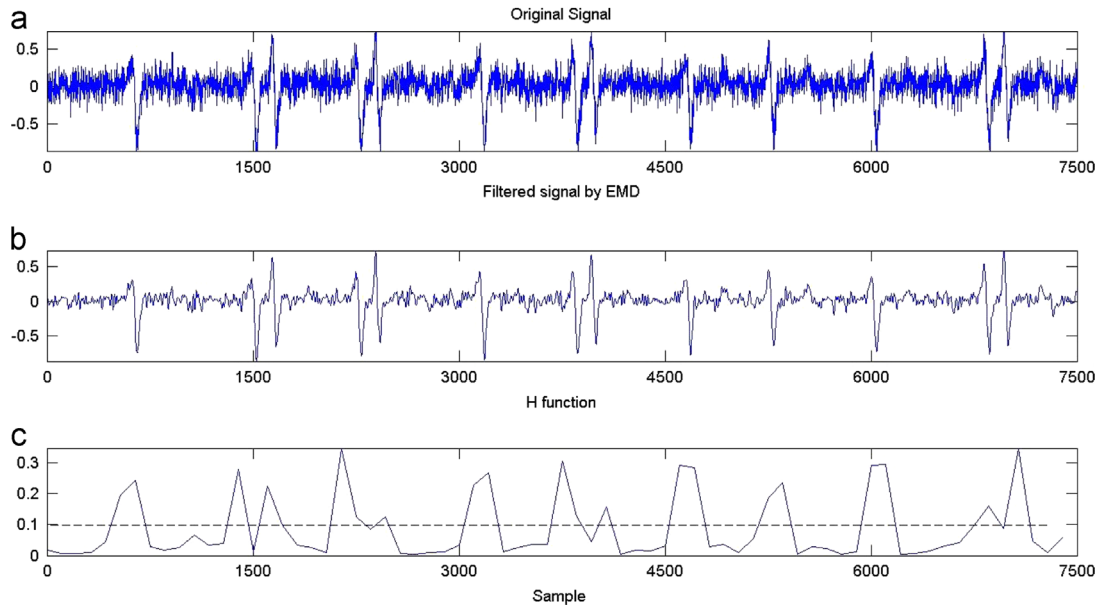


Fig. 19. Spike detection in test signal using standard deviation and EMD; (a) original signal, (b) decomposed signal after applying EMD, and (c) H function result. It can be seen that all 13 spikes can be accurately detected.

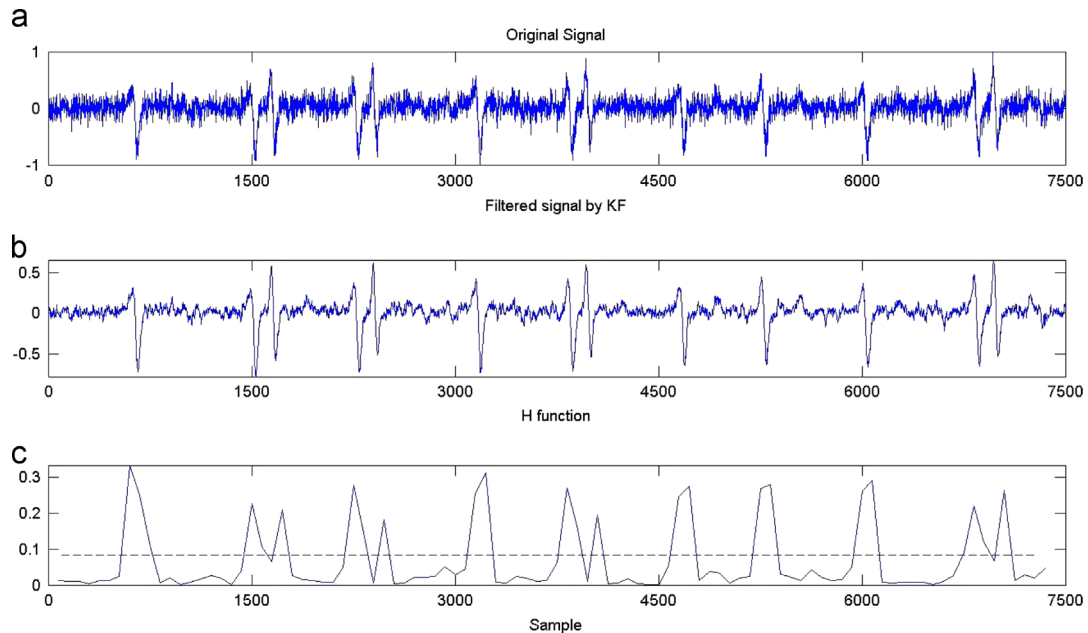


Fig. 20. Spike detection in test signal using standard deviation and KF; (a) original signal, (b) decomposed signal after applying KF, and (c) H function result. It can be seen that all 13 spikes can be accurately detected.

signal is smoother than the original signal. Fig. 10(c) illustrates the output of the filtered signal by SNEO method. As can be seen in Figs. 6(c), 7(c), 8(c), 9(c), and 10(c) the spikes for all 13 spikes can be accurately detected. Comparison between these figures and Fig. 4 demonstrates the effective of pre-processing steps for the SNEO method. Note all the utilized parameters for the SNEO methods are the same.

First, the Savitzky–Golay filter is applied for the test signal in Fig. 11. Since DWT can be a powerful tool for de-noising in biomedical signals, the test signal in Fig. 11(a) is decomposed using the four-level DWT with Daubechies wavelet of order eight. Fig. 12(c and d) illustrates the FD of the decomposed signal and changes in G function, respectively. Also, Figs. 13(d), 14(d), and 15(d) show G function by using SSA, EMD

and KF respectively as pre-processing steps. The parameters of the SSA, DWT, KF and Savitzky–Golay filter are selected exactly the same as ones are selected for the improved SNEO methods.

Fig. 16(a, b and c) show the test signal, the filtered signal by Savitzky–Golay, and the result of applying the standard deviation, respectively. As can be seen one spike is inaccurately detected. Figs. 17(c), 18(c), 19(c), and 20(c) show the attained outputs of applying the standard deviation with DWT, SSA, EMD, and KF, respectively. As can be seen in these figures, all 13 spikes are accurately detected. Therefore, for standard deviation, the DWT, SSA, EMD, and KF have better performance than Savitzky–Golay filter. Also, the parameters of DWT, SSA, KF and Savitzky–Golay filter are selected the same as ones are selected for the improved SNEO methods. In this paper for all

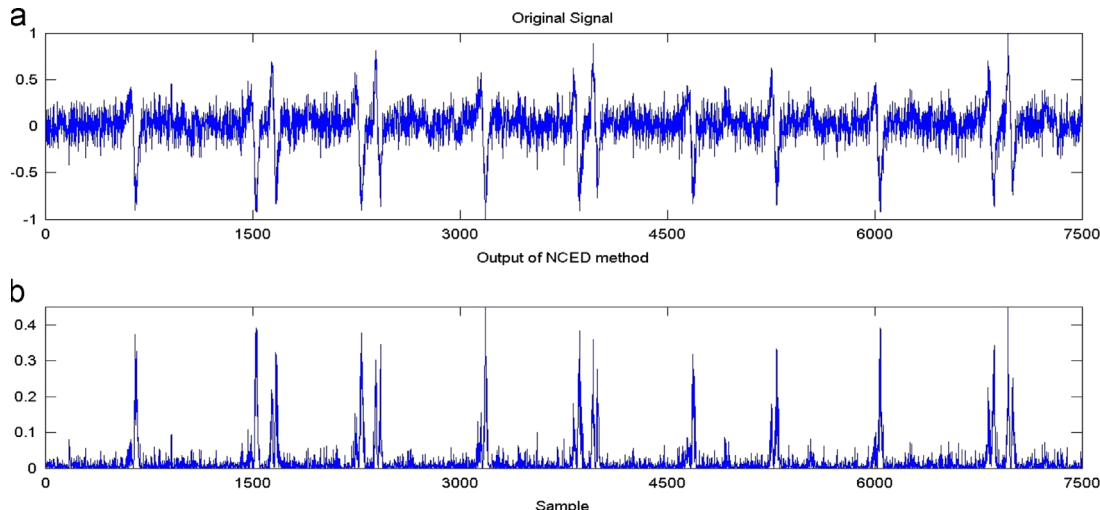


Fig. 21. Spike detection in test signal using NCED; (a) original signal, and (b) output of the NCED method.

mentioned methods, the mean value of the output is selected as the threshold. In Fig. 21(b), the output of NCED, as the best method proposed in [3], is shown. As can be seen, because of noise, the NCED detects some spikes incorrectly.

Three different parameters, namely, the true positive (TP) miss or false negative (FN) and false positive (FP) ratios were used to evaluate the performance and effectiveness of the proposed methods. These parameters are defined as

$$TP = (N_t/N), FN = (N_m/N), \text{ and } FP = (N_f/N). \quad (13)$$

where N_t , N_m and N_f represent the number of true, missed and falsely detected spikes respectively and N shows the actual number of spikes. In Table 1 the results of spike detection for the realistic synthetic data using the proposed methods with EMD, KF, SSA, DWT and Savitzky-Golay filter are shown. For a high SNR, the SNEO is a very good method to detect spikes, while the noises is increased, the performance of this method is reduced significantly. In order to overcome this problem, we use SSA, DWT, KF, EMD and Savitzky-Golay filter as pre-processing steps. As can be seen in Table 1, the performance of KF is approximately the same as Savitzky-Golay filter. The results show that DWT has a better performance than Savitzky-Golay filter and both of them can considerably improve spike detection methods.

As we can see in Table 1, when $\text{SNRs} > 0$, EMD performs best in terms of all the parameters. In addition, when $\text{SNRs} < 0$, SNEO with SSA is the best algorithm regarding to TPs and FNs not only among the SNEO-based methods but also among all the proposed methods.

Although TPs and FNs of spike detection with FD and DWT are the same as FD and Savitzky-Golay filter, attained FPs of spike detection method using FD and DWT is better than FD and Savitzky-Golay filter. The same as SNEO-based methods, SSA has better performance between all mentioned pre-processing algorithms among FD-based methods except EMD. In case of FP when SNR is low, FD with SSA is the best method between all the proposed methods.

The standard deviation with DWT can detect spikes better than the standard deviation with Savitzky-Golay filter/SSA. Also, among the standard deviation-based methods, only DWT as a pre-processing could detect all spikes with various SNRs. Therefore, the best method using standard deviation regarding to TPs and FNs is achieved using DWT. Also, unless standard deviation-based methods, the performance of SSA is better than DWT, KF and Savitzky-Golay filter. As can be seen in Table 2, although all of the methods have the acceptable consuming times except EMD, each method with DWT is clearly slower than one with SSA, KF and Savitzky-Golay filter. Savitzky-Golay is a bit quicker than SSA and KF. In this paper the simulations have been carried out using a

DELL-PC with Intel (R) Core (TM) i3 CPU M350 2.27 GHz and 2-GB RAM by MATLAB R2010a. In Table 2 we assess the CPU times for all mentioned methods. As can be seen in this table, the SNEO method is faster than spike detection using FD and the FD can detect spikes faster than spike detection using standard deviation.

Table 3 illustrates the comparison between SNEO with SSA and FD with SSA as two best proposed methods versus NCED as the best method between five suggested methods that were presented in [3]. As can be seen in this table, the proposed methods are much better than NCED.

It should be noted that applied methods in [3] have been used as a benchmark for comparison with many other methods. Also, the CPU time for NCED is about 0.034 s. Thus, although our proposed methods are not as fast as the NCED method, because these two proposed methods are enough fast for spike detection, we can ignore the CPU time problem.

In Table 4, comparison of spike detection rates for two best proposed methods and NCED for a part of the real external neuronal data can be viewed. The data is 900 s long and sampled at 20,000 samples/s taken from the CARMEN database. From the table, the best methods in terms of TP/FN and FP are improved SNEO by SSA and spike detection using FD and SSA, respectively. Both these methods are superior to NCED [3].

5. Conclusions

In this paper three new methods to detect the neuronal spikes buried in noise and interferences based on SNEO, FD and standard deviation have been proposed. Noises and short-term variations mixed in pure signals significantly reduce the performance of the spike detection methods. In order to overcome these problems and because DWT has low speed, SSA, KF and Savitzky-Golay filter have been used as pre-processing steps. Moreover, because DWT, SSA, KF and Savitzky-Golay filter have several parameters that must be adjusted by many trials, in this paper we have proposed the residual signal obtained by EMD. This residual signal has attained by taking out noises combined with original signal. The speeds of SSA, KF and Savitzky-Golay are much higher than that of DWT and EMD. Finally, by using the realistic synthetic and real neuronal data, the results attained by SNEO and SSA, and FD with SSA as two best proposed approaches have been compared with those of NCED, which is known as a powerful method for detecting spikes. It has been proved that the proposed approaches are superior and more effective in spike detection.

Table 1

Results of the suggested and improved methods on the realistic synthetic neuronal data.

Method	Parameters	–5 dB	0 dB	5 dB	10 dB	20 dB	50 dB
SNEO	TP (%)	40	48	64	84	98	100
	FN (%)	60	52	46	16	2	0
	FP (%)	184	147	98	54	18	0
Improved SNEO by DWT	TP (%)	96	96	100	100	100	100
	FN (%)	4	4	0	0	0	0
	FP (%)	48	30	0	0	0	0
Improved SNEO by Savitzky–Golay filter	TP (%)	96	96	100	100	100	100
	FN (%)	4	4	0	0	0	0
	FP (%)	53	24	2	0	0	0
Improved SNEO by SSA	TP (%)	100	100	100	100	100	100
	FN (%)	0	0	0	0	0	0
	FP (%)	27	8	2	0	0	0
Improved SNEO by EMD	TP (%)	79	91	100	100	100	100
	FN (%)	33	9	0	0	0	0
	FP (%)	81	39	0	0	0	0
Improved SNEO by KF	TP (%)	96	98	100	100	100	100
	FN (%)	4	2	0	0	0	0
	FP (%)	57	22	2	0	0	0
Spike detection using FD and DWT	TP (%)	96	98	100	100	100	100
	FN (%)	4	2	2	0	0	0
	FP (%)	46	18	2	0	0	0
Spike detection using FD and Savitzky–Golay filter	TP (%)	96	98	100	100	100	100
	FN (%)	4	2	0	0	0	0
	FP (%)	68	44	39	25	32	25
Spike detection using FD and SSA	TP (%)	98	98	98	100	100	100
	FN (%)	2	2	2	0	0	0
	FP (%)	11	18	4	12	4	2
Spike detection using FD and EMD	TP (%)	82	89	100	100	100	100
	FN (%)	18	11	0	0	0	0
	FP (%)	86	55	12	10	3	2
Spike detection using FD and KF	TP (%)	96	98	100	100	100	100
	FN (%)	4	2	0	0	0	0
	FP (%)	65	42	41	32	28	22
Spike detection using standard deviation and DWT	TP (%)	100	100	100	100	100	100
	FN (%)	0	0	0	0	0	0
	FP (%)	43	22	10	14	17	11
Spike detection using standard deviation and Savitzky–Golay filter	TP (%)	98	96	100	100	100	100
	FN (%)	2	4	0	0	0	0
	FP (%)	68	24	30	14	19	18
Spike detection using standard deviation and SSA	TP (%)	98	100	100	100	100	100
	FN (%)	2	0	0	0	0	0
	FP (%)	51	22	18	10	16	10
Spike detection using standard deviation and EMD	TP (%)	80	89	100	100	100	100
	FN (%)	20	11	0	0	0	0
	FP (%)	82	46	18	14	13	8
Spike detection using standard deviation and KF	TP (%)	96	98	98	100	100	100
	FN (%)	4	2	2	0	0	0
	FP (%)	64	25	28	17	16	15

Table 2

Comparison of CPU times for proposed methods.

Methods	CPU time (s)
Spike detection using standard deviation and DWT	0.417
Spike detection using standard deviation and Savitzky–Golay filter	0.128
Improved SNEO by DWT	0.193
Improved SNEO by Savitzky–Golay filter	0.054
SNEO	0.033
Spike detection using FD and DWT	0.385
Spike detection using FD and Savitzky–Golay filter	0.064
Improved SNEO by SSA	0.072
Spike detection using standard deviation and SSA	0.064
Spike detection using FD and SSA	0.071
Spike detection using standard deviation and KF	0.189
Improved SNEO by KF	0.132
Spike detection using FD and KF	0.121
Improved SNEO by EMD	about 15
Spike detection using standard deviation and EMD	about 15
Spike detection using FD and EMD	about 15

Table 3

Comparison of spike detection rates for two best proposed methods and NCED in realistic synthetic neuronal data.

Method	Parameters	−5 dB	0 dB	5 dB	10 dB	20 dB	50 dB
Improved SNEO by SSA	TP (%)	100	100	100	100	100	100
	FN (%)	0	0	0	0	0	0
	FP (%)	27	8	2	0	0	0
Spike detection using FD and SSA	TP (%)	98	98	98	100	100	100
	FN (%)	2	2	2	0	0	0
	FP (%)	11	18	4	12	4	2
NCED [3]	TP (%)	96	94	96	98	98	98
	FN (%)	4	6	4	2	2	2
	FP (%)	62	54	42	28	22	16

Table 4

Comparison of spike detection rates for two best proposed methods and NCED in real neuronal data.

Parameter	Improved SNEO by the SSA method	Spike detection using the FD and SSA method	NCED [3] method
TP (%)	94	91	89
FN (%)	6	9	11
FP (%)	17	12	21

Acknowledgment

The authors wish to thank Prof. Leslie S. Smith who gave real neuronal data. The authors are also grateful to Prof. Leslie S. Smith and Morteza Saraf for their valuable comments.

References

- [1] S. Shoham, M.R. Fellows, R.A. Normann, Robust, automatic spike sorting using mixtures of multivariate *t*-distributions, *J. Neurosci. Methods* 127 (2) (2003) 111–122.
- [2] A. Maccione, M. Gandolfo, P. Massobrio, A. Novellino, S. Martinoia, M. Chiappalone, A novel algorithm for precise identification of spikes in extracellularly recorded neuronal signals, *J. Neurosci. Methods* 177 (1) (2009) 241–249.
- [3] N. Mtetwa, L.S. Smith, Smoothing and thresholding in neuronal spike detection, *Neurocomputing* 69 (10–12) (2006) 1366–1370.
- [4] Z. Nenadic, J.W. Burdick, Spike detection using the continuous wavelet transform, *IEEE Trans. Biomed. Eng.* 52 (1) (2005) 74–87.
- [5] Y. Yuan, C. Yang, J. Si, An advanced spike detection and sorting system, in: Proceedings of International Joint Conference on Neural Networks, 2009, pp. 3477–3484.
- [6] X. Liu, X. Yang, N. Zheng, Automatic extracellular spike detection with piecewise optimal, *Neurocomputing* 79 (2012) 132–139.
- [7] S. Kim, J. McNames, Automatic spike detection based on adaptive template matching for extracellular neural recordings, *J. Neurosci. Methods* 165 (2) (2007) 165–174.
- [8] S. Shahid, J. Walker, L.S. Smith, A new spike detection algorithm for extracellular neural recordings, *IEEE Trans. Biomed. Eng.* 57 (4) (2010) 853–866.
- [9] S. Mukhopadhyay, G.C. Ray, A new interpretation of nonlinear energy operator and its efficiency in spike detection, *IEEE Trans. Biomed. Eng.* 49 (12) (2002) 1526–1533.
- [10] R. Esteller, G. Vachtsevanos, J. Echauz, B. litt, A comparison of waveform fractal dimension algorithms, *IEEE Trans. Circuits Syst.* 48 (2) (2001) 177–183.
- [11] H. Azami, S. Sanei, K. Mohammadi, A novel signal segmentation method based on standard deviation and variable threshold, *J. Comput. Appl. Math.* 34 (2) (2011) 27–34.
- [12] J. Gao, H. Sultan, J. Hu, W.W. Tung, Denoising nonlinear time series by adaptive filtering and wavelet shrinkage: a comparison, *IEEE Signal Process. Lett.* 17 (3) (2010) 237–240.
- [13] H. Azami, K. Mohammadi, B. Bozorgtabar, An improved signal segmentation using moving average and Savitzky–Golay filter, *J. Signal Inf. Process.* 3 (1) (2012) 39–44.
- [14] S. Sanei, T.K.M. Lee, V. Abolghasemi, A new adaptive line enhancer based on singular spectrum analysis, *IEEE Trans. Biomed. Eng.* 59 (2) (2012) 428–434.
- [15] N. Xiaoming, Z. Jian, L. Xingwu, Application of Hilbert–Huang transform to laser Doppler velocimeter, *Opt. Laser Technol.* 44 (7) (2012) 2197–2201.
- [16] K. Asaduzzaman, M.B.I. Reaz, F. Mohd-Yasin, K.S. Sim, M.S. Hussain, A study on discrete wavelet-based noise removal from EEG signals, *J. Adv. Exp. Med. Biol.* 680 (2010) 593–599.
- [17] E. Estrada, H. Nazeran, G. Sierra, F. Ebrahimi, S.K. Setarehdan, Wavelet-based EEG denoising for automatic sleep stage classification, in: Proceedings of International Conference on Electrical Communications and Computers, 2011, pp. 295–298.
- [18] Y. Tao, E.C.M. Lam, Y.Y. Tang, Feature extraction using wavelet and fractal, *Pattern Recognit.* 22 (3–4) (2001) 271–287.
- [19] S. Rajagopalan, J.M. Aller, J.A. Restrepo, T.G. Habetler, R.G. Harley, Analytic-wavelet-ridge-based detection of dynamic eccentricity in brushless direct current (BLDC) motors functioning under dynamic operating conditions, *IEEE Trans. Ind. Electron.* 54 (3) (2007) 1410–1419.
- [20] A. Savitzky, M.J.E. Golay, Smoothing and differentiation of data by simplified least square procedure, *Anal. Chem.* 36 (8) (1964) 1627–1639.
- [21] J. Lue, K. Ying, J. Bai, Savitzky–Golay smoothing and differentiation filter for even number data, *Signal Process.* 85 (7) (2005) 1429–1434.
- [22] H. Hassanpour, A time-frequency approach for noise reduction, *Digit. Signal Process.* 18 (5) (2008) 728–738.
- [23] H. Hassanpour, Singular spectrum analysis: methodology and comparison, *J. Data Sci.* 5 (2) (2007) 239–257.
- [24] F. Ghaderi, H. Mohseni, S. Sanei, Localizing heart sounds in respiratory signals using singular spectrum analysis, *IEEE Trans. Biomed. Eng.* 59 (12) (2011) 3360–3367.
- [25] H. Azami, S. Sanei, K. Mohammadi, H. Hassanpour, A hybrid evolutionary approach to segmentation of non-stationary signals, *Elsevier J. Digit. Signal Process.* 23 (4) (2013) 1103–1114.
- [26] M. Karimi-Ghartemani, M.R. Iravani, A nonlinear adaptive filter for on-line signal analysis in power systems: applications, *IEEE Trans. Power Deliv.* 17 (2) (2002) 617–622.
- [27] M. Karimi-Ghartemani, A.K. Ziarani, A nonlinear time frequency analysis method, *IEEE Trans. Signal Process.* 52 (2004) 1585–1595.
- [28] M.S. Grewal, A.P. Andrews, *Kalman Filtering: Theory and Practice using MATLAB*, 2nd ed., Wiley, New York, 2001.
- [29] S.M. Bozic, *Digital and Kalman Filtering: an Introduction to Discrete-Time Filtering and Optimal Linear Estimation*, Wiley, New York, 1983.
- [30] S.Z. Fana, Q. Wei, P.F. Shi, Y.J. Chenc, Q. Liub, J.S. Shieh, A comparison of patients' heart rate variability and blood flow variability during surgery based on the Hilbert–Huang transform, *Biomed. Signal Process. Control* 7 (5) (2012) 465–473.
- [31] J. Peng, G. Zhang, Analysis of signal characteristics of swirlmeter in oscillatory flow based on Hilbert–Huang transform (HHT), *Measurement* 45 (7) (2012) 1765–1781.
- [32] B.M. Battista, C. Knapp, T. McGee, V. Goebel, Application of the empirical mode decomposition and Hilbert–Huang transform to seismic reflection data, *Geophysics* 72 (2) (2007).
- [33] Y. Tao, E.C.M. Lam, Y.Y. Tang, Feature extraction using wavelet and fractal, *Elsevier J. Pattern Recognit.* 22 (3–4) (2001) 271–287.
- [34] U.R. Acharya, O. Faust, N. Kannathal, T. Chua, S. Laxminarayan, Non-linear analysis of EEG signals at various sleep stages, *Comput. Methods Programs Biomed.* 80 (1) (2005) 37–45.
- [35] J.F. Kaiser, On a simple algorithm to calculate the energy of a signal, in: proceedings of IEEE International Conference on Acoustics, Speech and Signal Processing, 1990, pp. 381–384.
- [36] H. Hassanpour, B. Boashash, A time-frequency approach for EEG spike detection, *Iran. J. Energy Environ.* 2 (4) (2011) 390–395.
- [37] L.S. Smith, N. Mtetwa, A tool for synthesizing spike trains with realistic interference, *J. Neurosci. Methods* 159 (1) (2007) 170–180.



Hamed Azami received his M.Sc. degree in Electronic Engineering from Department of Electrical Engineering, Iran University of Science and Technology, Tehran, Iran in 2011, as a top-ranked student. Currently, he is a lecturer in Electrical Engineering at Shomal University, Amol, Iran. His research interests include biomedical signal and image processing, and wireless communication systems.



Saeid Sanei received his Ph.D. degree in biomedical signal and image processing from Imperial College London, London, U.K. in 1991. He is an internationally known expert in signal processing, biomedical signal processing, and pattern recognition. He has published more than 280 refereed journal and conference papers. He published two books (research monograms) entitled "EEG Signal Processing" and "Adaptive Processing of Brain Signals" both with John Wiley publisher in 2007 and 2013 respectively. Currently, he is a reader in biomedical signal processing within Faculty of Engineering and Physical Sciences, University of Surrey, U.K.